Study of the sign change of the Sivers function from STAR collaboration W/Z production data

M. Anselmino,[a,b] **M. Boglione,**[a,b] **U. D'Alesio,**[c,d] **F. Murgia**[d] **and A. Prokudin**[e,f]

[a] *Dipartimento di Fisica Teorica, Università di Torino,*
  Via P. Giuria 1, I-10125 Torino, Italy

[b] *INFN — Sezione di Torino,*
  Via P. Giuria 1, I-10125 Torino, Italy

[c] *Dipartimento di Fisica, Università di Cagliari, Cittadella Universitaria,*
  I-09042 Monserrato CA, Italy

[d] *INFN — Sezione di Cagliari, Cittadella Universitaria,*
  I-09042 Monserrato CA, Italy

[e] *Science Division, Penn State University Berks,*
  Reading, Pennsylvania 19610, U.S.A.

[f] *Theory Center, Jefferson Lab,*
  12000 Jefferson Avenue, Newport News, VA 23606, U.S.A.

  E-mail: mauro.anselmino@to.infn.it, elena.boglione@to.infn.it, umberto.dalesio@ca.infn.it, francesco.murgia@ca.infn.it, prokudin@jlab.org

ABSTRACT: Recent data on the transverse single spin asymmetry A_N measured by the STAR Collaboration for $p^\uparrow p \to W^\pm/Z^0 X$ reactions at RHIC allow the first investigation of the Sivers function in Drell-Yan processes and of its expected sign change with respect to SIDIS processes. A new extraction of the Sivers functions from the latest SIDIS data is performed and a critical assessment of the significance of the STAR data is attempted.

Contents

1 Introduction

The Transverse Momentum Dependent Partonic Distribution Functions (TMD-PDFs) encode information on the 3-dimensional structure of nucleons in momentum space; they depend on the parton intrinsic motion inside the nucleon and, in general, on the nucleon and parton spins. At leading twist there are eight independent TMD-PDFs which have been studied in Semi Inclusive Deep Inelastic Scattering (SIDIS) processes. Among them, the Sivers distribution, which describes the momentum distribution of unpolarised quarks and gluons inside a transversely polarised proton, has a clear experimental signature [1, 2] and is of particular interest for several reasons; one expects it to be related to fundamental intrinsic features of the nucleon and to basic QCD properties.

In fact, the Sivers distribution $\Delta^N f_{q/p^\uparrow}$ relates the motion of unpolarised quarks and gluons to the nucleon spin $\boldsymbol{S}$; then, in order to build a scalar, parity invariant quantity, $\boldsymbol{S}$ must couple to the only other available pseudo-vector, that is the parton orbital angular momentum, $\boldsymbol{L}_q$ or $\boldsymbol{L}_g$. Another peculiar feature of the Sivers distribution is that its origin at partonic level can be traced in QCD interactions between the quarks (or gluons) active in inelastic high energy interactions and the nucleon remnants [3, 4]; thus, it is expected to be process dependent and have opposite signs in SIDIS and Drell-Yan (D-Y) processes [5, 6]:

$$\Delta^N f_{q/p^\uparrow}(x, k_\perp)|_{\mathrm{SIDIS}} = -\Delta^N f_{q/p^\uparrow}(x, k_\perp)|_{\mathrm{D-Y}}. \tag{1.1}$$

This important prediction remains to be tested.

The Sivers distribution can be accessed through the study of azimuthal asymmetries in polarised SIDIS and Drell-Yan (D-Y) processes. These have been clearly observed in the last years, in SIDIS, by the HERMES [1], COMPASS [2] and Jefferson Lab [7] Collaborations, allowing extractions of the SIDIS Sivers function [8–11]. However, no information could be obtained on the D-Y Sivers function, as no polarised D-Y process had ever been measured.

Recently, first data from polarised D-Y processes at RHIC, $p^\uparrow p \to W^\pm/Z^0 X$, have become available [12]. The data show an azimuthal asymmetry, A_N^W, which can be interpreted as due to the Sivers effect and which hints [12, 13] at a sign change between the Sivers function observed in these D-Y processes and the Sivers function extracted from SIDIS processes. However, considering the importance of the sign change issue, before drawing any definite conclusion, both the SIDIS and D-Y data and their comparison, have to be critically analysed and discussed.

In this paper we perform a new extraction of the valence and sea-quark Sivers functions from the newest experimental SIDIS data. We then perform an analysis of the RHIC $W^\pm/Z^0$ D-Y data [12], based on these new functions, trying to assess the significance of A_N^W on the sign change of the Sivers functions.

The paper is organised as follows: in section 2 we recall the formalism used to analyse and interpret the experimental data. In section 3 we present a new extraction of the Sivers functions from experimental data. In section 4 we compute the asymmetries observable in D-Y processes and based on the SIDIS extracted Sivers functions, both with and without the sign change; we compare them with the recent RHIC results and comment on the significance of the D-Y data as a possible indication of the sign change of the Sivers function. Conclusions and final comments are given in section 5.

2 Formalism

We consider a generalised Drell-Yan process, $p^\uparrow p \to W^\pm X$, in which one observes a W boson, with four-momentum q, created by the annihilation of a quark and an antiquark. We define our kinematical configuration with the polarised $p^\uparrow$ proton, with four-momentum p_1, moving along the positive z-axis and the unpolarised one, with four-momentum p_2, moving opposite to it. We adopt the usual variables:

$$q = (q_0, \boldsymbol{q}_T, q_L) \qquad q^2 = M_W^2 \qquad y_W = \frac{1}{2}\ln\frac{q_0 + q_L}{q_0 - q_L} \qquad x_F = \frac{2\,q_L}{\sqrt{s}} \qquad s = (p_1 + p_2)^2\,. \tag{2.1}$$

The annihilating quarks have an intrinsic transverse motion, $\boldsymbol{k}_{\perp 1}$ and $\boldsymbol{k}_{\perp 2}$. We fix the azimuthal angles by choosing the "up" ($\uparrow$) polarisation direction as the positive y-axis ($\phi_S = \pi/2$). The spin "down"($\downarrow$) polarisation direction will have $\phi_S = 3\pi/2$. The other transverse momenta azimuthal angles are defined as:

$$\boldsymbol{q}_T = q_T(\cos\phi_W,\,\sin\phi_W,\,0) \qquad \boldsymbol{k}_{\perp i} = k_{\perp i}(\cos\varphi_i,\,\sin\varphi_i,\,0) \qquad (i=1,2)\,. \tag{2.2}$$

In the kinematical region

$$q_T^2 \ll M_W^2 \qquad k_\perp \simeq q_T\,, \tag{2.3}$$

using the TMD factorisation formalism at leading order, the unpolarised cross section for the $p\,p \to W\,X$ process can be written as [13–16]

$$\frac{d\sigma^{pp\to WX}}{dy_W\,d^2\boldsymbol{q}_T} = \hat\sigma_0 \sum_{q_1,q_2} |V_{q_1,q_2}|^2 \int d^2\boldsymbol{k}_{\perp 1}\,d^2\boldsymbol{k}_{\perp 2}\,\delta^2(\boldsymbol{k}_{\perp 1} + \boldsymbol{k}_{\perp 2} - \boldsymbol{q}_T)\,f_{q_1/p}(x_1, k_{\perp 1})\,f_{q_2/p}(x_2, k_{\perp 2})\,, \tag{2.4}$$

where $f_{q_i/p}(x_i, k_{\perp i})$ are the unpolarised TMDs, V_{q_1,q_2} are the weak interaction CKM matrix elements and the $\sum_{q_1,q_2}$ runs over all appropriate light quark and antiquark flavours ($q_1 q_2 = u\bar{d}, \bar{d}u, u\bar{s}, \bar{s}u$ for W^+, etc.). $\hat{\sigma}_0$ is the lowest-order partonic cross section (with G_F the Fermi weak coupling constant),

$$\hat{\sigma}_0 = \frac{\sqrt{2}\,\pi\, G_F\, M_W^2}{3\, s}\,, \tag{2.5}$$

and the parton longitudinal momentum fractions are given, at $\mathcal{O}\left(k_\perp / M_W\right)$, by

$$x_{1,2} = \frac{M_W}{\sqrt{s}}\, e^{\pm y_W} = \frac{\pm x_F + \sqrt{x_F^2 + 4\, M_W^2/s}}{2}\,. \tag{2.6}$$

Notice that, with the definition of x_F adopted in eq. (2.1), one has

$$x_F = x_1 - x_2 \qquad\qquad |x_F| \le 1 - \frac{M_W^2}{s}\,. \tag{2.7}$$

In such a formalism, the distribution for unpolarised quarks with transverse momentum $\boldsymbol{k}_\perp$ inside a proton with 3-momentum $\boldsymbol{p}$ and spin $\boldsymbol{S}$,

$$\begin{aligned}
\hat{f}_{q/p^\uparrow}(x, \boldsymbol{k}_\perp) &= f_{q/p}(x, k_\perp) + \frac{1}{2}\, \Delta^N f_{q/p^\uparrow}(x, k_\perp)\, \boldsymbol{S} \cdot (\hat{\boldsymbol{p}} \times \hat{\boldsymbol{k}}_\perp) \\
&= f_{q/p}(x, k_\perp) - \frac{k_\perp}{m_p}\, f_{1T}^{\perp q}(x, k_\perp)\, \boldsymbol{S} \cdot (\hat{\boldsymbol{p}} \times \hat{\boldsymbol{k}}_\perp)\,,
\end{aligned} \tag{2.8}$$

generates a transverse Single Spin Asymmetry (SSA)

$$A_N^W = \frac{d\sigma^{p^\uparrow p \to WX} - d\sigma^{p^\downarrow p \to WX}}{d\sigma^{p^\uparrow p \to WX} + d\sigma^{p^\downarrow p \to WX}} \equiv \frac{d\sigma^\uparrow - d\sigma^\downarrow}{d\sigma^\uparrow + d\sigma^\downarrow}\,, \tag{2.9}$$

$$\begin{aligned}
d\sigma^\uparrow - d\sigma^\downarrow = \hat{\sigma}_0 \sum_{q_1, q_2} |V_{q_1,q_2}|^2 \int d^2\boldsymbol{k}_{\perp 1}\, d^2\boldsymbol{k}_{\perp 2}\, \delta^2(\boldsymbol{k}_{\perp 1} + \boldsymbol{k}_{\perp 2} - \boldsymbol{q}_T) \\
\times\, \boldsymbol{S} \cdot (\hat{\boldsymbol{p}}_1 \times \hat{\boldsymbol{k}}_{\perp 1})\, \Delta^N f_{q_1/p^\uparrow}(x_1, k_{\perp 1})\, f_{q_2/p}(x_2, k_{\perp 2})\,, \quad (2.10)
\end{aligned}$$

$$\begin{aligned}
d\sigma^\uparrow + d\sigma^\downarrow = 2\hat{\sigma}_0 \sum_{q_1, q_2} |V_{q_1,q_2}|^2 \int d^2\boldsymbol{k}_{\perp 1}\, d^2\boldsymbol{k}_{\perp 2}\, \delta^2(\boldsymbol{k}_{\perp 1} + \boldsymbol{k}_{\perp 2} - \boldsymbol{q}_T) \\
\times\, f_{q_1/p}(x_1, k_{\perp 1})\, f_{q_2/p}(x_2, k_{\perp 2})\,. \quad (2.11)
\end{aligned}$$

where $d\sigma$ stands for $d\sigma^{pp \to WX}/(dy_W\, d^2\boldsymbol{q}_T)$ and $\Delta^N f_{q/p^\uparrow}(x, k_\perp)$ is the Sivers function.

The above expression much simplifies adopting, as usual, a Gaussian factorised form both for the unpolarised distribution and the Sivers functions, as in ref. [8]:

$$f_{q/p}(x, k_\perp) = f_q(x)\, \frac{1}{\pi \langle k_\perp^2 \rangle}\, e^{-k_\perp^2 / \langle k_\perp^2 \rangle}\,, \tag{2.12}$$

$$\Delta^N f_{q/p^\uparrow}(x, k_\perp) = 2\, \mathcal{N}_q(x)\, h(k_\perp)\, f_{q/p}(x, k_\perp)\,, \tag{2.13}$$

$$\mathcal{N}_q(x) = N_q\, x^{\alpha_q}(1-x)^{\beta_q}\, \frac{(\alpha_q + \beta_q)^{(\alpha_q + \beta_q)}}{\alpha_q^{\alpha_q}\, \beta_q^{\beta_q}}\,, \tag{2.14}$$

$$h(k_\perp) = \sqrt{2e}\, \frac{k_\perp}{M_1}\, e^{-k_\perp^2 / M_1^2}\,, \tag{2.15}$$

where $f_q(x)$ are the unpolarised PDFs, M_1 is a parameter which allows the $k_\perp$ Gaussian dependence of the Sivers function to be different from that of the unpolarised TMDs and $\mathcal{N}_q(x)$ is a function which parameterises the factorised x dependence of the Sivers function.

The following moment of the Sivers function is of importance:

$$\Delta^N f_{q/p^\uparrow}^{(1)}(x) = \int d^2 \boldsymbol{k}_\perp \frac{k_\perp}{4m_p} \Delta^N f_{q/p^\uparrow}(x, k_\perp) = -f_{1T}^{\perp(1)q}(x) , \qquad (2.16)$$

$$\Delta^N f_{q/p^\uparrow}^{(1)}(x) = \frac{\sqrt{\frac{e}{2}} \langle k_\perp^2 \rangle M_1^3}{m_p(\langle k_\perp^2 \rangle + M_1^2)^2} \mathcal{N}_q(x) f_q(x) . \qquad (2.17)$$

With the choices of eqs. (2.12)–(2.15) the $\boldsymbol{k}_\perp$ integrations can be performed analytically in eq. (2.11), obtaining:

$$A_N^W(y_W, \boldsymbol{q}_T) = \boldsymbol{S} \cdot (\hat{\boldsymbol{p}}_1 \times \hat{\boldsymbol{q}}_T) \frac{2 \langle k_S^2 \rangle^2}{[\langle k_S^2 \rangle + \langle k_\perp^2 \rangle]^2} \exp\left[-\frac{q_T^2}{2 \langle k_\perp^2 \rangle} \left(\frac{\langle k_\perp^2 \rangle - \langle k_S^2 \rangle}{\langle k_\perp^2 \rangle + \langle k_S^2 \rangle} \right) \right] \frac{\sqrt{2e} \, q_T}{M_1}$$

$$\times \frac{\sum_{q_1,q_2} |V_{q_1,q_2}|^2 \mathcal{N}_{q_1}(x_1) f_{q_1}(x_1) f_{q_2}(x_2)}{\sum_{q_1,q_2} |V_{q_1,q_2}|^2 f_{q_1}(x_1) f_{q_2}(x_2)} \qquad (2.18)$$

$$\equiv \cos\phi_W \, A_N(y_W, q_T) \qquad (2.19)$$

with

$$\langle k_S^2 \rangle = \frac{M_1^2 \langle k_\perp^2 \rangle}{M_1^2 + \langle k_\perp^2 \rangle} \qquad (2.20)$$

and where, in the last line, we have used, according to our kinematics, $\boldsymbol{S} \cdot (\hat{\boldsymbol{p}}_1 \times \hat{\boldsymbol{q}}_T) = \cos\phi_W$. $A_N(y_W, q_T)$ is the quantity measured at RHIC [12].[1]

Let us notice that the RHIC measurements of $W^\pm$ production at $\sqrt{s} = 500\,\text{GeV}$ [12] cover the rapidity region $|y_W| < 1$. In particular, data are available for $y_W \simeq \pm 0.4$ and $y_W \simeq 0$. This corresponds to:

$$
\begin{array}{llll}
y_W \simeq -0.4 & \quad x_1 \simeq 0.11 & \quad x_2 \simeq 0.24 & \\
y_W \simeq 0 & \quad x_1 \simeq 0.16 & \quad x_2 \simeq 0.16 & \quad (2.21) \\
y_W \simeq +0.4 & \quad x_1 \simeq 0.24 & \quad x_2 \simeq 0.11 , &
\end{array}
$$

where x_1 refers to the polarised proton and x_2 to the unpolarised one. Then, although the x region is predominantly the valence one, the data at $y_W \simeq -0.4$ are expected to be more sensitive to the sea-quark Sivers functions.

3 Extraction of Sivers functions from SIDIS data

The quark flavours involved in W production include anti-quarks. Thus, in order to estimate the asymmetry A_N^W, it is important to have a reliable extraction of both quark and anti-quark Sivers functions.

---

[1]Notice that in ref. [12] there is a deceptive definition of $\cos\phi$, which is opposite to ours. However, we have checked with the STAR Collaboration that the quantity measured is exactly that defined in eq. (2.19).

For instance, in order to produce a W^+, u, $\bar{d}$ and $\bar{s}$ quarks from the polarised proton combine with $\bar{d}$, $\bar{s}$, u quarks from the unpolarised proton, such that the asymmetry is proportional to

$$|V_{u,d}|^2 \left(\Delta^N f_{u/p^\uparrow} \otimes f_{\bar{d}/p} + \Delta^N f_{\bar{d}/p^\uparrow} \otimes f_{u/p} \right) + |V_{u,s}|^2 \left(\Delta^N f_{u/p^\uparrow} \otimes f_{\bar{s}/p} + \Delta^N f_{\bar{s}/p^\uparrow} \otimes f_{u/p} \right). \tag{3.1}$$

Both quantities in the round brackets in the above equation contain a sea and a valence quark distribution. However, because of the numerical values[2] of $|V_{u,d}|$ and $|V_{u,s}|$, the last two terms in eq. (3.1) are much suppressed with respect to the first two. Thus, we expect that $A_N^{W^+}$ mainly depends on the u quark and $\bar{d}$ sea quark Sivers functions.

Likewise, for W^- production, the asymmetry is proportional to

$$|V_{u,d}|^2 \left(\Delta^N f_{\bar{u}/p^\uparrow} \otimes f_{d/p} + \Delta^N f_{d/p^\uparrow} \otimes f_{\bar{u}/p} \right) + |V_{u,s}|^2 \left(\Delta^N f_{\bar{u}/p^\uparrow} \otimes f_{s/p} + \Delta^N f_{s/p^\uparrow} \otimes f_{\bar{u}/p} \right), \tag{3.2}$$

and we expect that W^- data are mainly sensitive to d quark and $\bar{u}$ sea quark Sivers function.

A previous extraction of the Sivers functions that included anti-quark distributions was reported in ref. [8]. However, new data have become available since then and we perform here a new complete extraction of the Sivers functions. We refer to ref. [8] for more details about the procedure.

One may notice that in our simple parameterisation of the Sivers functions as given in eqs. (2.12)–(2.15) the knowledge of the width $\langle k_\perp^2 \rangle$ of the unpolarised TMDs is important. Such a study was performed in refs. [18, 19]. We adopt here the parameters from ref. [18], fixed by fitting the HERMES multiplicities [20]:

$$\langle k_\perp^2 \rangle = 0.57 \pm 0.08 \text{ GeV}^2 \qquad \langle p_\perp^2 \rangle = 0.12 \pm 0.01 \text{ GeV}^2 \,, \tag{3.3}$$

where $\langle p_\perp^2 \rangle$ is the width of unpolarised Transverse Momentum Dependent Fragmentation Functions (TMD-FFs):

$$D_{h/q}(z, p_\perp) = D_{h/q}(z) \frac{1}{\pi \langle p_\perp^2 \rangle} e^{-p_\perp^2 / \langle p_\perp^2 \rangle} \,. \tag{3.4}$$

Notice that the study of ref. [18] found no flavour dependence of the widths of the TMDs. The collinear distribution and fragmentation functions, $f_{q/p}(x)$ and $D_{h/q}(z)$, needed for our parameterisations are taken from the available fits of the world data: in this analysis we use the CTEQ6L set for the PDFs [21] and the DSS set for the fragmentation functions [22]. The LHAPDF [23] library is used for collinear PDFs. We fit the latest data from the HERMES Collaboration on the SIDIS Sivers asymmetries for $\pi^\pm$ and $K^\pm$ production off a proton target [1], the COMPASS Collaboration data on LiD [24] and NH$_3$ targets [25], and JLab data on ^{3}He target [26].

These available SIDIS data cover a relatively narrow region of x, typically in the so-called valence region. It suffices to use the most simple parameterisation for the anti-quark Sivers functions [see eqs. (2.13), (2.14)]:

$$\mathcal{N}_{\bar{q}}(x) = N_{\bar{q}} \,. \tag{3.5}$$

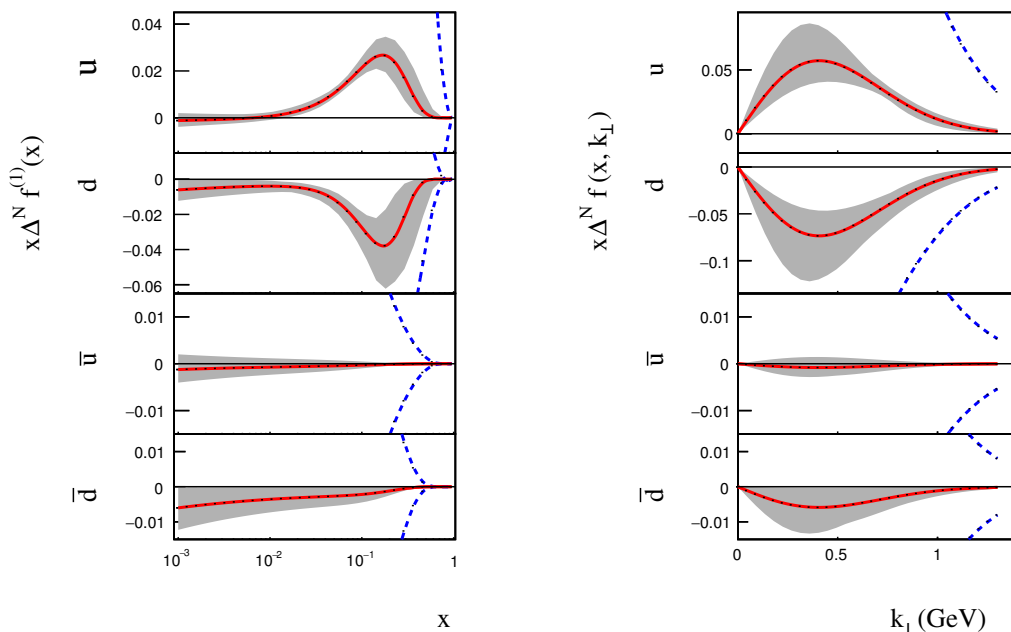[2]$|V_{u,d}| = 0.97417 \pm 0.00021$, $|V_{u,s}| = 0.2248 \pm 0.0006$, from ref. [17].

Figure 1. Extracted Sivers distributions for $u = u_v + \bar{u}$, $d = d_v + \bar{d}$, $\bar{u}$ and $\bar{d}$ at $Q^2 = 2.4\,\text{GeV}^2$. Left panel: the first moment of the Sivers functions, eqs. (2.16) and (2.17) of the text, versus x. Right panel: plots of the Sivers functions, eq. (2.14) of the text, at $x = 0.1$ versus $k_\perp$. The solid lines correspond to the best fit. The dashed lines correspond to the positivity bound of the Sivers functions. The shaded bands correspond to our estimate of 95% C.L. error.

It means that we assume the anti-quark Sivers functions to be proportional to the corresponding unpolarised PDFs; we have checked that a fit allowing for more complicated structures of eq. (2.14) for the anti-quarks, results in undefined values of the parameters α and β.

The Sivers asymmetry measured in SIDIS can be expressed using our parameterisations of TMD functions from eqs. (2.12)–(2.15), (3.4) as

$$A_{UT}^{\sin(\phi_h - \phi_S)}(x, y, z, P_T) = \frac{[z^2 \langle k_\perp^2 \rangle + \langle p_\perp^2 \rangle] \langle k_S^2 \rangle^2}{[z^2 \langle k_S^2 \rangle + \langle p_\perp^2 \rangle]^2 \langle k_\perp^2 \rangle} \exp\left[- \frac{P_T^2 z^2 (\langle k_\perp^2 \rangle - \langle k_S^2 \rangle)}{(z^2 \langle k_S^2 \rangle + \langle p_\perp^2 \rangle)(z^2 \langle k_\perp^2 \rangle + \langle p_\perp^2 \rangle)} \right]$$
$$\times \frac{\sqrt{2\,e}\, z\, P_T}{M_1} \frac{\sum_q e_q^2 \mathcal{N}_q(x) f_q(x)\, D_{h/q}(z)}{\sum_q e_q^2 f_q(x)\, D_{h/q}(z)} \,. \tag{3.6}$$

Thus, we introduce a total of 9 free parameters for valence and sea-quark Sivers functions: N_{u_v}, N_{d_v}, $N_{\bar{u}}$, $N_{\bar{d}}$, α_u, β_u, α_d, β_d, and M_1^2 (GeV^2). In order to estimate the errors on the parameters and on the calculation of the asymmetries we follow the Monte Carlo sampling method explained in ref. [8]. That is, we generate samples of parameters $\boldsymbol{\alpha}_i$, where each $\boldsymbol{\alpha}_i$ is an array of random values of $\{N_{u_v}, N_{d_v}, N_{\bar{u}}, N_{\bar{d}}, \alpha_u, \alpha_d, \beta_u, \beta_d, M_1^2\}$, in the vicinity of the minimum found by MINUIT, $\boldsymbol{\alpha}_0$, that defines the minimal total χ^2 value, $\chi_{\min}^2$. We generate $2 \cdot 10^4$ sets of parameters $\boldsymbol{\alpha}_i$ that satisfy

$$\chi^2(\boldsymbol{\alpha}_i) \leq \chi_{\min}^2 + \Delta\chi^2 \,, \tag{3.7}$$

N_{u_v}	=	$0.18 \pm 0.01 (\pm 0.04)$	α_{u_v}	=	$1.0 \pm 0.3 (\pm 0.6)$	β_{u_v}	=	$6.6 \pm 2.0 (\pm 5.2)$
N_{d_v}	=	$-0.52 \pm 0.08 (\pm 0.20)$	α_{d_v}	=	$1.9 \pm 0.5 (\pm 1.5)$	β_{d_v}	=	$10. \pm 4.0 (\pm 11.)$
$N_{\bar{u}}$	=	$-0.01 \pm 0.01 (\pm 0.03)$					
$N_{\bar{d}}$	=	$-0.06 \pm 0.02 (\pm 0.06)$					
M_1^2	=	$0.8 \pm 0.2 (\pm 0.9)$ (GeV^2)					
$\chi^2_{\min} = 325.29$			$\chi^2_{\min}/\text{dof} = 1.29$				

Table 1. Fitted parameters of the Sivers valence quark and anti-quark distributions for u_v, d_v, $\bar{u}$, $\bar{d}$. The fit is performed by using MINUIT minimisation package. Quoted errors correspond to MINUIT estimate with $\Delta\chi^2 = 1$, and $\Delta\chi^2 = 17.21$ for errors in parentheses.

with the high tolerance $\Delta\chi^2 = 17.21$ that corresponds to the 95% C.L. of coverage probability for 9 free parameters. The fit is performed with MINUIT minimisation package and the resulting parameters can be found in table 1; the corresponding extracted Sivers functions are shown in figure 1. We indicate both the errors for the standard definition of $\Delta\chi^2 = 1$ and the high tolerance error with $\Delta\chi^2 = 17.21$ (the errors given in parentheses).

The main new features of the fit are the parameters $N_{d_v} = -0.52 \pm 0.20$ and $N_{u_v} = 0.18 \pm 0.04$. The previous extraction [8], that used different gaussian width values, $\langle k_\perp^2 \rangle = 0.25$ GeV^2 and $\langle p_\perp^2 \rangle = 0.20$ GeV^2, yielded $N_d = -0.9$, which almost saturated the positivity bound $|N_q| = 1$, and $N_u = 0.35$. The $\bar{u}$ and $\bar{d}$ Sivers functions turn out to be both small, compared to the quark distributions, and negative. Future Electron-Ion Collider data will be crucial for the investigation of the anti-quark Sivers distributions. The parameters that control the large-x behaviour of the functions, β_{u_v} and β_{d_v}, have big errors, see table 1. The future Jefferson Lab 12 GeV data will allow a better precision extraction in the high-x region.

The partial contributions to χ^2 from different experiments are shown in table 2. One can see that the proton data on π^+ from the HERMES Collaboration and the positive hadron data from the COMPASS Collaboration show some larger χ^2 values that might be attributed to possible effects of TMD evolution [10, 11, 27].

Several plots showing the quality of our best fits of the data are presented in figure 2.

4 Predictions for W and Z asymmetries and comparison with data

We can now compute the asymmetry $A_N(y_W, q_T)$, according to eqs. (2.18)–(2.19), using the Sivers functions — *or their opposite* — as given in eqs. (2.12)–(2.15) with the parameters, and the corresponding uncertainties, shown in table 1.

Actually, in order to compare with data [12], we integrate both the numerator and denominator of A_N^W, eqs. (2.10)–(2.11), either over q_T in the region $[0.5, 10]$ GeV, or over y_W from -1 to 1. The results, *reversing the sign of the SIDIS extracted Sivers functions as in eq. (1.1)*, are shown and compared with data respectively in figure 3 and in figure 4. For completeness, despite the much limited amount and quality of data, we also show our

Experiment	Hadron	Target	Dependence	ndata	χ^2	χ^2/ndata
JLAB [26]	π^+	^{3}He	x	4	2.24	0.56
JLAB [26]	π^-	^{3}He	x	4	3.50	0.87
HERMES [1]	π^0	H	x	7	5.63	0.80
HERMES [1]	π^+	H	x	7	18.72	2.67
HERMES [1]	π^-	H	x	7	14.82	2.12
HERMES [1]	π^0	H	z	7	7.43	1.06
HERMES [1]	π^+	H	z	7	4.26	0.61
HERMES [1]	π^-	H	z	7	4.60	0.66
HERMES [1]	π^0	H	P_T	7	5.85	0.84
HERMES [1]	π^+	H	P_T	7	17.13	2.45
HERMES [1]	π^-	H	P_T	7	6.62	0.95
HERMES [1]	K^+	H	x	7	8.90	1.27
HERMES [1]	K^-	H	x	7	4.46	0.64
HERMES [1]	K^+	H	z	7	9.94	1.42
HERMES [1]	K^-	H	z	7	8.49	1.21
HERMES [1]	K^+	H	P_T	7	8.38	1.20
HERMES [1]	K^-	H	P_T	7	5.70	0.81
COMPASS [24]	π^+	LiD	x	9	3.09	0.34
COMPASS [24]	π^-	LiD	x	9	4.75	0.53
COMPASS [24]	π^+	LiD	z	8	6.30	0.79
COMPASS [24]	π^-	LiD	z	8	10.86	1.36
COMPASS [24]	π^+	LiD	P_T	9	5.94	0.66
COMPASS [24]	π^-	LiD	P_T	9	4.65	0.52
COMPASS [24]	K^+	LiD	x	9	8.13	0.90
COMPASS [24]	K^-	LiD	x	9	12.02	1.34
COMPASS [24]	K^+	LiD	z	8	9.70	1.21
COMPASS [24]	K^-	LiD	z	8	9.39	1.17
COMPASS [24]	K^+	LiD	P_T	9	6.40	0.71
COMPASS [24]	K^-	LiD	P_T	9	15.10	1.68
COMPASS [25]	h^+	NH$_3$	x	9	33.76	3.75
COMPASS [25]	h^-	NH$_3$	x	9	12.14	1.35
COMPASS [25]	h^+	NH$_3$	z	8	16.56	2.07
COMPASS [25]	h^-	NH$_3$	z	8	14.87	1.86
COMPASS [25]	h^+	NH$_3$	P_T	9	8.29	0.92
COMPASS [25]	h^-	NH$_3$	P_T	9	12.41	1.38

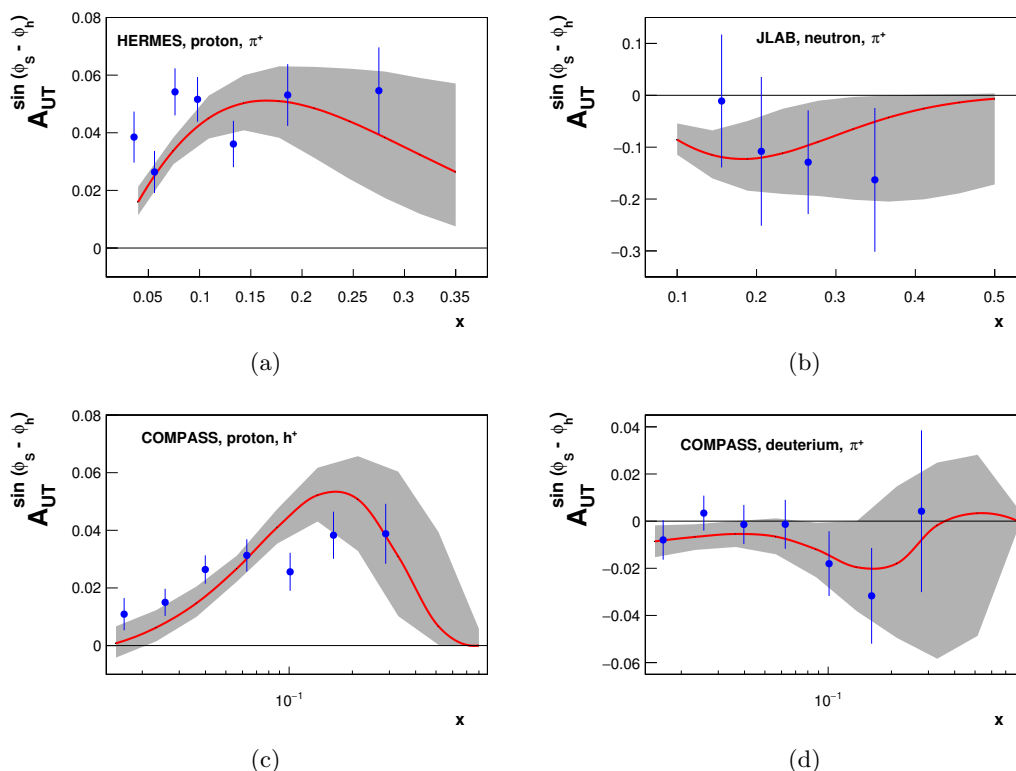**Table 2**. Partial χ^2 values of the global best fit for SIDIS experiments.

Figure 2. Examples of best fits of SIDIS experimental data: (a) Data from the HERMES Collaboration for π^+ production off hydrogen target as function of x. (b) Data from JLab 6 for π^+ production off ^{3}He target as function of x. (c) Data from the COMPASS Collaboration for h^+ production off NH$_3$ target as function of x. (d) Data from the COMPASS Collaboration for π^+ production off LiD target as function of x. The solid lines correspond to the best fit. The shaded region corresponds to our estimate of 95% C.L. error band.

estimate of A_N, integrated over q_T, for Z^0 production, in figure 5. The results *without the sign change* can be easily deduced by reversing the sign of the asymmetry in figures 3–5.

Before trying a quantitative evaluation of the significance of the data regarding the issue of the sign change of the Sivers function going from SIDIS to D-Y processes, a few comments are in order.

- In general, the agreement between our estimates and the few data is rather poor, both with and without sign change. In particular, this is evident from the q_T dependence of A_N, figure 4, and the y_z dependence of A_N for Z^0, figure 5. In the latter case there is only one single data point, with a big error, indicating a large positive asymmetry.

- The data on the y_W dependence are given by collecting all W's produced with q_T up to $10\,\text{GeV}$. The simple model of D-Y TMD factorisation including only DGLAP evolution that we use in this analysis is expected to hold for lower values of q_T; integrating the theoretical results up to such values, in order to compare with the available data, is a somewhat ambiguous procedure. Implementation of the TMD
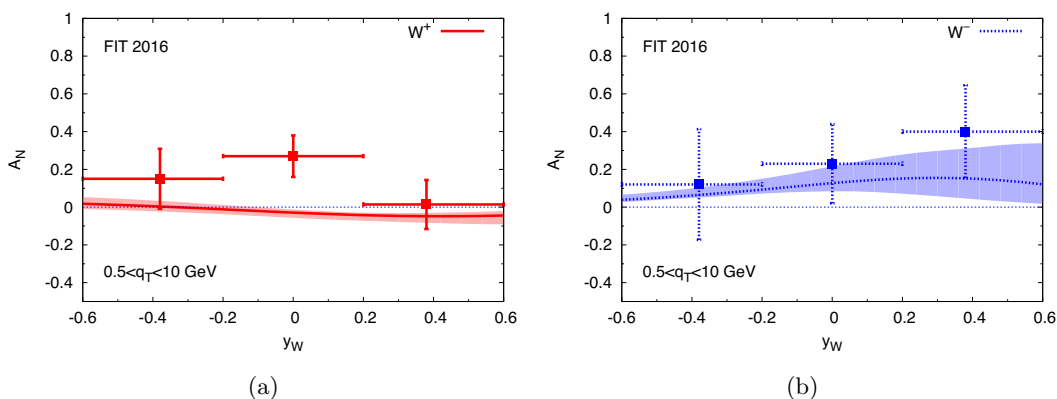
Figure 3. Our estimates of the Sivers asymmetry A_N for W^+ (a) and W^- (b) production, assuming a sign change of the SIDIS Sivers functions, compared with the experimental data as function of y_W. q_T is integrated in the region $[0.5, 10]$ GeV.
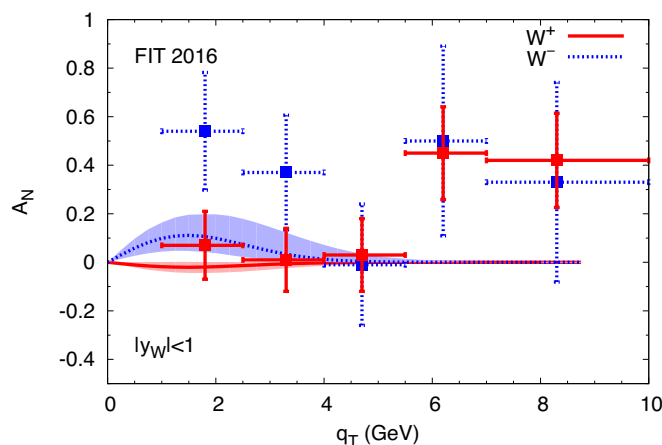

Figure 4. Our estimates of the Sivers asymmetry A_N for W^+ and W^- production, assuming a sign change of the SIDIS Sivers functions, compared with the experimental data as function of q_T. y_W is integrated in the region $[-1, 1]$.

evolution would not help to make the agreement with the data better in this case, as TMD evolution predicts a suppression of the asymmetries for higher values of Q^2 with respect to the initial lower scale [11]. This suppression might become moderate depending on the shape of the non-perturbative input of TMD evolution [28–30].

- Considering the q_T integrated data, from a first look at figure 3 it appears that indeed W^- data are compatible with the sign change, while W^+ data may be compatible with either sign of the Sivers functions.

- The shape of the TMDs and the values of the parameters here adopted allow a good description of the SIDIS data; however, they are still rather flexible, and our numerical estimates for the D-Y asymmetry might depend on the choice, for example, of the values of the Gaussian width, eq. (3.3). A full study of combined unpolarised SIDIS, D-Y and (future) e^+e^- data is mandatory.
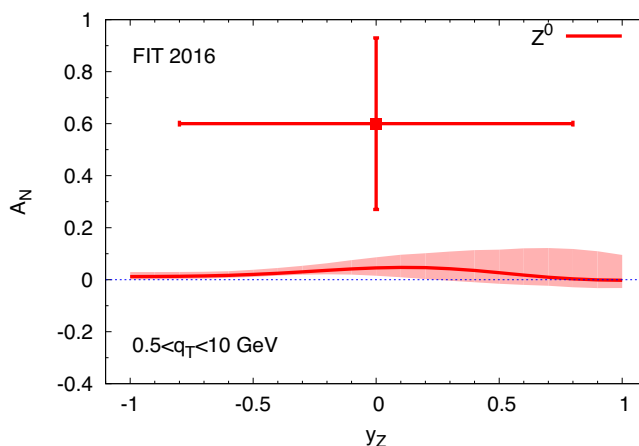
Figure 5. Our estimate of the Sivers asymmetry A_N for Z^0 production, assuming a sign change of the SIDIS Sivers functions, compared with the experimental data as function of y_z. q_T is integrated in the region $[0.5, 10]\,\mathrm{GeV}$.

Aware of the above comments, we may still take at face value the RHIC data on A_N for $W^\pm$ production and try to quantify their impact on the extraction of the Sivers function. That is, we calculate the deviation between the data and our estimates, separately for W^+ and W^-:

$$\chi^2(\boldsymbol{\alpha}) = \sum_{n=1}^{\mathrm{dof}} \left(\frac{[\text{theory}]_n(\boldsymbol{\alpha}) - [\exp]_n}{[\Delta\exp]_n} \right)^2 , \qquad (4.1)$$

where $[\text{theory}]_n(\boldsymbol{\alpha})$ corresponds to the calculation of the W asymmetry using the phenomenological extraction of the Sivers function performed in this paper, with model parameters $\boldsymbol{\alpha}$, with and without the sign change of eq. (1.1); $[\exp]_n$ are the data for W^+ or W^- asymmetries and $[\Delta\exp]_n$ are the corresponding experimental errors. As we explained in section 3, in order to estimate the error on the extraction of the Sivers functions, we generate $2 \cdot 10^4$ sets of parameters $\boldsymbol{\alpha}$ according to eq. (3.7). Thus, we calculate $2 \cdot 10^4$ values of χ^2 using eq. (4.1) for W^+ and W^-. The histogram of all these values of χ^2/dof are shown in figure 6, where dof = 8 is the number of experimental points in each set for $W^\pm$. The green histogram corresponds to χ^2 with no sign change of the Sivers function, while the blue histogram corresponds to χ^2 with the sign change of the Sivers functions.

One can see from the upper left panel of figure 6 that W^- data favour the sign change: in this case the values of χ^2/dof are around 1.1, while without the sign change they are around 2.7. The W^+ data on the other hand are slightly better with no sign change, as can be seen from the upper right panel of figure 6. For either scenarios the χ^2 per number of data are rather large: these large values are due to the single point at $y_W = 0$ (see figure 3, left panel) and the two points at large $q_T > 5\,\mathrm{GeV}$ (see figure 4).

If we combine both W^+ and W^- data, then the two data sets globally favour a sign change of the Sivers functions according to eq. (1.1). The histogram of the combined data sets is presented in the lower panel of figure 6. If one assumes no sign change, then $\langle \chi^2/\mathrm{dof} \rangle = 2.35$ and $\sigma(\chi^2/\mathrm{dof}) = 0.1$, where dof = 16, while the sign change yields a
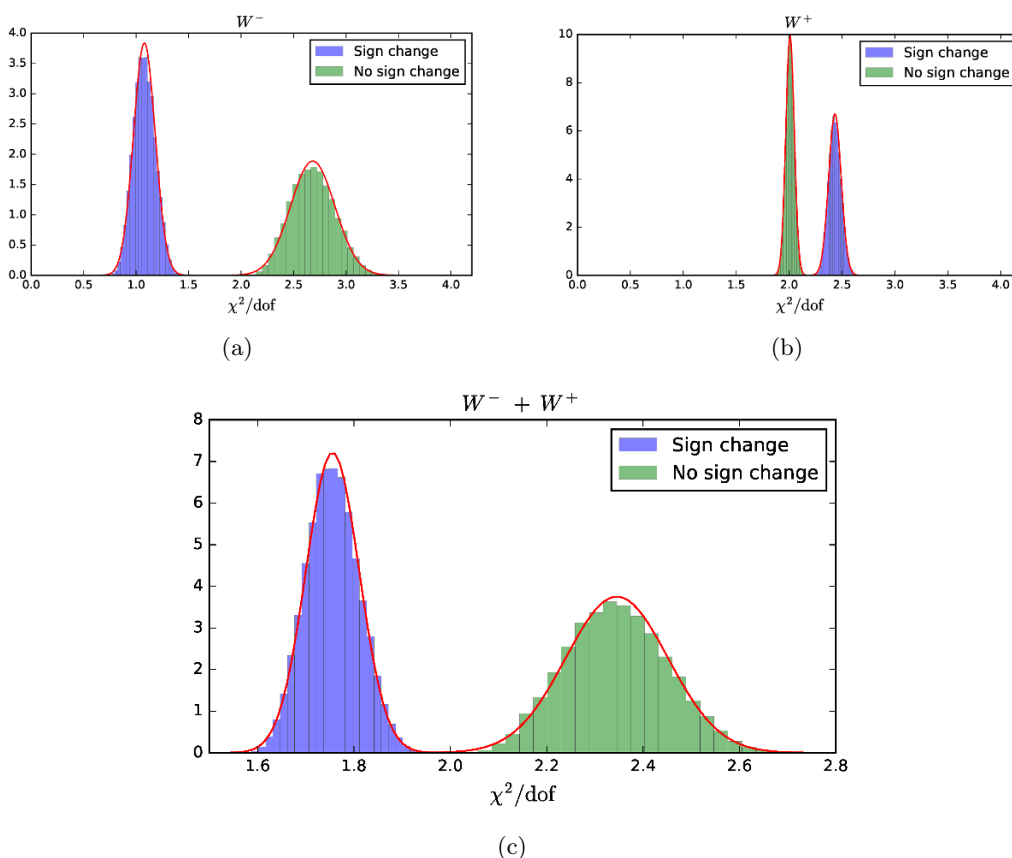
Figure 6. (a),(b): probability density functions of the χ^2/dof separately for our predictions of W^- (left) and W^+ (right) asymmetries, obtained from all parameter sets used to calculate the error band. The green histograms correspond to no sign change of the Sivers function, while the blue histograms correspond to the sign change. Fitted normal distributions are shown as solid lines. (c): probability density functions of the χ^2/dof, as in the upper plots, but globally for our predictions of $W^- + W^+$ asymmetries.

lower value, $\langle \chi^2/\mathrm{dof} \rangle = 1.75$ and $\sigma(\chi^2/\mathrm{dof}) = 0.05$. Notice that both scenarios have some disagreement with our estimates: indeed the values of χ^2/dof are well above one. Using our results from figure 6 we can at most conclude that $W^\pm$ data hint at an indication of the sign change according to eq. (1.1).

5 Comments and conclusions

We have analysed the recent data on the single spin asymmetry A_N^W measured by the STAR Collaboration at RHIC [12]; it is the first ever spin asymmetry measured in Drell-Yan processes and it might originate from the fundamental Sivers distribution of polarised quarks in an unpolarised proton. Then, it could help in testing the validity of the widely expected sign change of the Sivers function when extracted in SIDIS and D-Y processes, eq. (1.1).

In order to perform an unbiased analysis we have re-derived, by best fitting the latest SIDIS data [1, 24–26], the Sivers functions, including the anti-quark ones which might play a role in the D-Y production of Ws and Z^0s. Our results are shown in tables 1 and 2 and in figure 1.

Using the newly extracted Sivers SIDIS functions we have computed the D-Y SSA A_N for $W^\pm$ and Z^0 production, both with and without a sign change of the Sivers functions. Then, we have compared our results with the STAR data, figures 3–5, trying to assess their significance with respect to the sign change issue. Our quantitative results, according to eq. (4.1), can be seen in figure 6.

As commented throughout the paper, our simple model of D-Y TMD factorisation without evolution, eqs. (2.9)–(2.15), is, in general, in poor agreement with the data. A more refined analysis, using the TMD evolution, would probably worsen the agreement [11]. One should add that the data, although important and pioneering, are still scarce, with large errors, and gathered in different kinematical regions.

With all the necessary caution, from our analysis of the data, one can at most conclude that, only from W^- production, there is an indication in favour of the sign change of the Sivers function, which, however, is still far from being considered as proven. Soon expected data from COMPASS polarised D-Y processes, $\pi^- p^\uparrow \to \ell^+ \ell^- X$, and higher statistics data from STAR Collaboration on W and Z production should add important information.

Acknowledgments

References

[1] HERMES collaboration, A. Airapetian et al., *Observation of the naive-T-odd Sivers effect in deep-inelastic scattering*, *Phys. Rev. Lett.* **103** (2009) 152002 [`arXiv:0906.3918`] [INSPIRE].

[2] COMPASS collaboration, C. Adolph et al., *II — Experimental investigation of transverse spin asymmetries in μ-p SIDIS processes: Sivers asymmetries*, *Phys. Lett.* **B 717** (2012) 383 [`arXiv:1205.5122`] [INSPIRE].

[3] S.J. Brodsky, D.S. Hwang and I. Schmidt, *Final state interactions and single spin asymmetries in semiinclusive deep inelastic scattering*, *Phys. Lett.* **B 530** (2002) 99 [`hep-ph/0201296`] [INSPIRE].

[4] S.J. Brodsky, D.S. Hwang and I. Schmidt, *Initial state interactions and single spin asymmetries in Drell-Yan processes*, *Nucl. Phys.* **B 642** (2002) 344 [`hep-ph/0206259`] [INSPIRE].

[5] J.C. Collins, *Leading twist single transverse-spin asymmetries: Drell-Yan and deep inelastic scattering*, *Phys. Lett.* **B 536** (2002) 43 [`hep-ph/0204004`] [ɪɴSPIRE].

[6] S.J. Brodsky, D.S. Hwang, Y.V. Kovchegov, I. Schmidt and M.D. Sievert, *Single-spin asymmetries in semi-inclusive deep inelastic scattering and Drell-Yan processes*, *Phys. Rev.* **D 88** (2013) 014032 [`arXiv:1304.5237`] [ɪɴSPIRE].

[7] JEFFERSON LAB HALL A collaboration, K. Allada et al., *Single spin asymmetries of inclusive hadrons produced in electron scattering from a transversely polarized ^3He target*, *Phys. Rev.* **C 89** (2014) 042201 [`arXiv:1311.1866`] [ɪɴSPIRE].

[8] M. Anselmino et al., *Sivers effect for pion and kaon production in semi-inclusive deep inelastic scattering*, *Eur. Phys. J.* **A 39** (2009) 89 [`arXiv:0805.2677`] [ɪɴSPIRE].

[9] A. Bacchetta and M. Radici, *Constraining quark angular momentum through semi-inclusive measurements*, *Phys. Rev. Lett.* **107** (2011) 212001 [`arXiv:1107.5755`] [ɪɴSPIRE].

[10] M. Anselmino, M. Boglione and S. Melis, *A strategy towards the extraction of the Sivers function with TMD evolution*, *Phys. Rev.* **D 86** (2012) 014028 [`arXiv:1204.1239`] [ɪɴSPIRE].

[11] M.G. Echevarria, A. Idilbi, Z.-B. Kang and I. Vitev, *QCD evolution of the Sivers asymmetry*, *Phys. Rev.* **D 89** (2014) 074013 [`arXiv:1401.5078`] [ɪɴSPIRE].

[12] STAR collaboration, L. Adamczyk et al., *Measurement of the transverse single-spin asymmetry in $p^\uparrow + p \to W^\pm/Z^0$ at RHIC*, *Phys. Rev. Lett.* **116** (2016) 132301 [`arXiv:1511.06003`] [ɪɴSPIRE].

[13] J. Huang, Z.-B. Kang, I. Vitev and H. Xing, *Spin asymmetries for vector boson production in polarized $p + p$ collisions*, *Phys. Rev.* **D 93** (2016) 014036 [`arXiv:1511.06764`] [ɪɴSPIRE].

[14] M. Anselmino, M. Boglione, U. D'Alesio, S. Melis, F. Murgia and A. Prokudin, *Sivers effect in Drell-Yan processes*, *Phys. Rev.* **D 79** (2009) 054010 [`arXiv:0901.3078`] [ɪɴSPIRE].

[15] Z.-B. Kang and J.-W. Qiu, *Testing the time-reversal modified universality of the Sivers function*, *Phys. Rev. Lett.* **103** (2009) 172001 [`arXiv:0903.3629`] [ɪɴSPIRE].

[16] J.-C. Peng and J.-W. Qiu, *Novel phenomenology of parton distributions from the Drell-Yan process*, *Prog. Part. Nucl. Phys.* **76** (2014) 43 [`arXiv:1401.0934`] [ɪɴSPIRE].

[17] PARTICLE DATA GROUP collaboration, K.A. Olive et al., *Review of particle physics*, *Chin. Phys.* **C 38** (2014) 090001 [ɪɴSPIRE].

[18] M. Anselmino, M. Boglione, J.O. Gonzalez Hernandez, S. Melis and A. Prokudin, *Unpolarised transverse momentum dependent distribution and fragmentation functions from SIDIS multiplicities*, *JHEP* **04** (2014) 005 [`arXiv:1312.6261`] [ɪɴSPIRE].

[19] A. Signori, A. Bacchetta, M. Radici and G. Schnell, *Investigations into the flavor dependence of partonic transverse momentum*, *JHEP* **11** (2013) 194 [`arXiv:1309.3507`] [ɪɴSPIRE].

[20] HERMES collaboration, A. Airapetian et al., *Multiplicities of charged pions and kaons from semi-inclusive deep-inelastic scattering by the proton and the deuteron*, *Phys. Rev.* **D 87** (2013) 074029 [`arXiv:1212.5407`] [ɪɴSPIRE].

[21] J. Pumplin, D.R. Stump, J. Huston, H.L. Lai, P.M. Nadolsky and W.K. Tung, *New generation of parton distributions with uncertainties from global QCD analysis*, *JHEP* **07** (2002) 012 [`hep-ph/0201195`] [ɪɴSPIRE].

[22] D. de Florian, R. Sassot and M. Stratmann, *Global analysis of fragmentation functions for pions and kaons and their uncertainties*, *Phys. Rev.* **D 75** (2007) 114010 [`hep-ph/0703242`] [ɪɴSPIRE].

[23] A. Buckley et al., *LHAPDF6: parton density access in the LHC precision era*, *Eur. Phys. J.* **C 75** (2015) 132 [arXiv:1412.7420] [INSPIRE].

[24] COMPASS collaboration, M. Alekseev et al., *Collins and Sivers asymmetries for pions and kaons in muon-deuteron DIS*, *Phys. Lett.* **B 673** (2009) 127 [arXiv:0802.2160] [INSPIRE].

[25] COMPASS collaboration, C. Adolph et al., *Collins and Sivers asymmetries in muonproduction of pions and kaons off transversely polarised protons*, *Phys. Lett.* **B 744** (2015) 250 [arXiv:1408.4405] [INSPIRE].

[26] JEFFERSON LAB HALL A collaboration, X. Qian et al., *Single spin asymmetries in charged pion production from semi-inclusive deep inelastic scattering on a transversely polarized ^3He target*, *Phys. Rev. Lett.* **107** (2011) 072003 [arXiv:1106.0363] [INSPIRE].

[27] S.M. Aybat, A. Prokudin and T.C. Rogers, *Calculation of TMD evolution for transverse single spin asymmetry measurements*, *Phys. Rev. Lett.* **108** (2012) 242003 [arXiv:1112.4423] [INSPIRE].

[28] C.A. Aidala, B. Field, L.P. Gamberg and T.C. Rogers, *Limits on transverse momentum dependent evolution from semi-inclusive deep inelastic scattering at moderate Q*, *Phys. Rev.* **D 89** (2014) 094002 [arXiv:1401.2654] [INSPIRE].

[29] J. Collins and T. Rogers, *Understanding the large-distance behavior of transverse-momentum-dependent parton densities and the Collins-Soper evolution kernel*, *Phys. Rev.* **D 91** (2015) 074020 [arXiv:1412.3820] [INSPIRE].

[30] Z.-B. Kang, A. Prokudin, P. Sun and F. Yuan, *Extraction of quark transversity distribution and collins fragmentation functions with QCD evolution*, *Phys. Rev.* **D 93** (2016) 014009 [arXiv:1505.05589] [INSPIRE].